The Impact of Stratospheric Ozone Recovery on the Southern Hemisphere Westerly Jet

means that the energy barrier to charge injection from the gold contacts must be smaller than the 0.7 eV E_F-E_{HOMO} offset measured by ultraviolet photoelectron spectroscopy (UPS) (20). Indeed, the offset will be reduced considerably by both the image potential associated with the metal contacts and the polaron shift (16), both of which are not accounted for in UPS measurements (37).

The negative slope in the high-voltage regime III' of Fig. 4D suggests that field emission may also occur in OPI 10 (similar results were obtained for OPI 6 to 9). From the slope in regime III', we calculated the emission barrier height (ϕ_{FE}) to be in the range of 0.3 to 0.5 eV, assuming carrier effective mass ratios in the range 0.1 to 1.0, which are typical for molecular junctions (24). We also considered other possible transport mechanisms in the metal/wire/metal junction, such as Schottky emission at the contact, Poole-Frenkel emission in the wires, and space-charge-limited transport in the presence of traps (38, 39). However, we did not obtain reasonable values for extracted physical parameters with these other mechanisms (20). The estimated emission barrier heights for the other long OPI wires are also listed in Table 1 and table S1. Regime II' is a transitional regime between ohmic conduction and field emission for OPI 10, and it may correspond to space-charge-limited conduction (SCLC), based on the slope of 2.6 in the log I versus log V plot (Fig. 4B) and the slope of -3.5 in the log I versus log L plot at 0.7 V (inset in Fig. 4B) (39, 40). Further work is necessary to conclusively establish the transport mechanism in this regime.

References and Notes

1. A. Nitzan, M. A. Ratner, *Science* **300**, 1384 (2003).
2. W. B. Davis, W. A. Svec, M. A. Ratner, M. R. Wasielewski, *Nature* **396**, 60 (1998).
3. B. Giese, J. Amaudrut, A. K. Kohler, M. Spormann, S. Wessely, *Nature* **412**, 318 (2001).
4. R. L. Carroll, C. B. Gorman, *Angew. Chem. Int. Ed.* **41**, 4378 (2002).
5. H. D. Sikes et al., *Science* **291**, 1519 (2001).
6. J. He et al., *J. Am. Chem. Soc.* **127**, 1384 (2005).
7. K. S. Kwok, J. C. Ellenbogen, *Mater. Today* **5**, 28 (2002).
8. D. Segal, A. Nitzan, W. B. Davis, M. R. Wasielewski, M. A. Ratner, *J. Phys. Chem. B* **104**, 3817 (2000).
9. D. Segal, A. Nitzan, M. Ratner, W. B. Davis, *J. Phys. Chem. B* **104**, 2790 (2000).
10. Y. A. Berlin, A. L. Burin, M. A. Ratner, *Chem. Phys.* **275**, 61 (2002).
11. B. Giese, *Acc. Chem. Res.* **33**, 631 (2000).
12. E. M. Conwell, *Proc. Natl. Acad. Sci. U.S.A.* **102**, 8795 (2005).
13. D. N. Beratan, J. N. Onuchic, J. R. Winkler, H. B. Gray, *Science* **258**, 1740 (1992).
14. H. B. Gray, J. R. Winkler, *Proc. Natl. Acad. Sci. U.S.A.* **102**, 3534 (2005).
15. W. P. Hu et al., *Phys. Rev. Lett.* **96**, 027801 (2006).
16. S. Kubatkin et al., *Nature* **425**, 698 (2003).
17. Y. Selzer, M. A. Cabassi, T. S. Mayer, D. L. Allara, *J. Am. Chem. Soc.* **126**, 4052 (2004).
18. Y. Selzer et al., *Nano Lett.* **5**, 61 (2005).
19. J. J. W. M. Rosink et al., *Langmuir* **16**, 4547 (2000).
20. Materials and methods are available as supporting material on *Science* Online.
21. D. J. Wold, C. D. Frisbie, *J. Am. Chem. Soc.* **123**, 5549 (2001).
22. V. B. Engelkes, J. M. Beebe, C. D. Frisbie, *J. Am. Chem. Soc.* **126**, 14287 (2004).
23. X. D. Cui et al., *Science* **294**, 571 (2001).
24. A. Salomon et al., *Adv. Mater.* **15**, 1881 (2003).
25. M. D. Newton, *Chem. Rev.* **91**, 767 (1991).
26. F. C. Grozema, Y. A. Berlin, L. D. A. Siebbeles, *J. Am. Chem. Soc.* **122**, 10903 (2000).
27. Y. L. Shen, A. R. Hosseini, M. H. Wong, G. G. Malliaras, *Chem. Phys. Chem.* **5**, 16 (2004).
28. R. Akaba, K. Tokumaru, T. Kobayashi, *Bull. Chem. Soc. Jpn.* **53**, 1993 (1980).
29. J. Harada, M. Harakawa, K. Ogawa, *Acta Crystallogr. B* **60**, 578 (2004).
30. T. Tsuji, H. Takeuchi, T. Egawa, S. Konaka, *J. Am. Chem. Soc.* **123**, 6381 (2001).
31. F. C. Grozema et al., *Adv. Mater.* **14**, 228 (2002).
32. F. C. Grozema, P. T. van Duijnen, Y. A. Berlin, M. A. Ratner, L. D. A. Siebbeles, *J. Phys. Chem. B* **106**, 7791 (2002).
33. P. Prins et al., *Phys. Rev. Lett.* **96**, 146601 (2006).
34. Y. A. Berlin, G. R. Hutchison, P. Rempala, M. A. Ratner, J. Michl, *J. Phys. Chem. A* **107**, 3970 (2003).
35. Y. A. Berlin, M. A. Ratner, *Radiat. Phys. Chem.* **74**, 124 (2005).
36. J. M. Beebe, B.-S. Kim, J. W. Gadzuk, C. D. Frisbie, J. G. Kushmerick, *Phys. Rev. Lett.* **97**, 026801 (2006).
37. X.-Y. Zhu, *Surf. Sci. Rep.* **56**, 1 (2004).
38. S. M. Sze, *Physics of Semiconductor Devices* (Wiley, New York, 1981).
39. M. A. Lampert, *Phys. Rev.* **103**, 1648 (1956).
40. A. Rose, *Phys. Rev.* **97**, 1538 (1955).
41. J. M. Tour et al., *J. Am. Chem. Soc.* **117**, 9529 (1995).
42. The authors thank G. Haugstad for support in the temperature-dependent measurements and X.-Y. Zhu for help with photoelectron spectroscopy. This work was supported primarily by the National Science Foundation under CHE-0616427. Partial support for facilities was provided by the NSF Materials Research Science and Engineering Centers program under DMR-0212302. Parts of this work were carried out in the Institute of Technology Characterization Facility, University of Minnesota, which receives partial support from NSF through the National Nanotechnology Infrastructure Network program.

The Impact of Stratospheric Ozone Recovery on the Southern Hemisphere Westerly Jet

S.-W. Son,[1]* L. M. Polvani,[1,2] D. W. Waugh,[3] H. Akiyoshi,[4] R. Garcia,[5] D. Kinnison,[5] S. Pawson,[6] E. Rozanov,[7,8] T. G. Shepherd,[9] K. Shibata[10]

In the past several decades, the tropospheric westerly winds in the Southern Hemisphere have been observed to accelerate on the poleward side of the surface wind maximum. This has been attributed to the combined anthropogenic effects of increasing greenhouse gases and decreasing stratospheric ozone and is predicted to continue by the Intergovernmental Panel on Climate Change/Fourth Assessment Report (IPCC/AR4) models. In this paper, the predictions of the Chemistry-Climate Model Validation (CCMVal) models are examined: Unlike the AR4 models, the CCMVal models have a fully interactive stratospheric chemistry. Owing to the expected disappearance of the ozone hole in the first half of the 21st century, the CCMVal models predict that the tropospheric westerlies in Southern Hemisphere summer will be decelerated, on the poleward side, in contrast with the prediction of most IPCC/AR4 models.

Recent observations (1–4) indicate that the westerly jet in the Southern Hemisphere (SH) troposphere is accelerating on the poleward side; this is usually described as a positive trend of the Southern annular mode index (1). This acceleration has important consequences for SH climate: It directly affects the surface temperatures (2), the extent of sea ice (2), the variability of storm tracks (5), the location of arid regions (6), the strength of the wind-driven oceanic circulation (7), and the exchange of CO_2 and heat between atmosphere and ocean (7, 8).

Understanding and predicting changes in the SH westerlies are therefore of the utmost importance.

Climate models have shown that the recent wind changes likely result from an increase in greenhouse gases and the depletion of stratospheric ozone (9–11), but the relative contribution of these two effects remains an open question, especially for the 21st century when stratospheric ozone is expected to recover as a result of the implementation of the Montreal Protocol (12). The multimodel mean of the IPCC/AR4 atmosphere-ocean–coupled model integrations indicates that the acceleration of the SH westerlies on the

[1]Department of Applied Physics & Applied Mathematics, Columbia University, New York, NY 10027, USA. [2]Department of Earth and Environmental Sciences, Columbia University, New York, NY 10027, USA. [3]Department of Earth and Planetary Sciences, Johns Hopkins University, Baltimore, MD 21218, USA. [4]National Institute for Environmental Studies, Tsukuba, Japan. [5]National Center for Atmospheric Research (NCAR), Boulder, CO 80325, USA. [6]NASA/Goddard Space Flight Center, Greenbelt, MD 20771, USA. [7]Institute for Atmospheric and Climate Sciences/Eidgenössische Technische Hochschule (ETH), Zurich, Switzerland. [8]Physical Meteorological Observatory, World Radiation Center, Davos, Switzerland. [9]Department of Physics, University of Toronto, Toronto, Canada. [10]Meteorological Research Institute, Tsukuba, Japan.

*To whom correspondence should be addressed. E-mail: sws2112@columbia.edu

poleward side will continue in the 21st century (5, 13, 14), albeit at a weaker rate (13). However, because ozone recovery is not uniformly specified among the AR4 models, it is unclear at present what role, if any, ozone recovery plays in the acceleration of the SH westerlies.

To explore this issue, we examine the predictions of the CCMVal activity of the "stratospheric processes and their role in climate" (SPARC) project (15). These models faithfully reproduce past climate change in the SH (see the supporting online material). In this study, we analyze the output of all seven CCMVal models, which performed integrations up to the year 2050 (16). In contrast to AR4 models described below, the CCMVal models have a high vertical resolution in the stratosphere, a model top located above the stratopause (~ 50 km), and fully interactive stratospheric chemistry. All CCMVal models are forced with the IPCC A1B scenario for greenhouse gases and Ab scenario for halogen concentrations. The sea surface temperature is prescribed from either the coupled AR4 model on which a given

CCMVal model is based or the UK Meteorological Office Hadley Centre model output (15).

The CCMVal model integrations are contrasted with those of AR4 models forced by A1B scenario greenhouse gases (17). Although the two sets of model integrations are comparable in the troposphere, they are substantially different in the stratosphere. Most AR4 models have the model top well below the stratopause (17, 18). More importantly, time changes in stratospheric ozone concentration are ignored by nearly half the models. We examine the output of all 19 AR4 models, which is available at the IPCC/AR4 data archive: Of these models, 10 prescribe stratospheric ozone recovery, and the other 9 do not (19). The ozone recovery in the former group is specified either as simple linear function of time or from the output of two-dimensional models, which are driven by halogen loading consistent with the Montreal Protocol (17). The detailed spatial and temporal structures of the prescribed ozone recovery, however, have not been documented.

Because stratospheric ozone is predicted to increase approximately linearly from 2001 to 2050 in almost all CCMVal model integrations (15, 20), we compute linear trends of all quantities using monthly or seasonally averaged zonal fields, from 2001 to 2050. Trends are first calculated for the individual model realizations with a least-square fit and then averaged among all available ensemble members for the same model. The multimodel mean trend in the spatial domain is produced by interpolating each model's trend linearly to the latitudes and log-linearly to the pressure levels.

We start by considering how ozone recovery affects the temperature in the upper troposphere and lower stratosphere. Figure 1A shows the SH polar-cap ozone trend predicted by multimodel mean of CCMVal models. The strongest ozone recovery is found at 50 hPa in October and at lower altitudes in the following months. This pattern is largely reminiscent of ozone depletion in the recent past (21, 22), except for the reversal in sign and slightly higher location of maximum
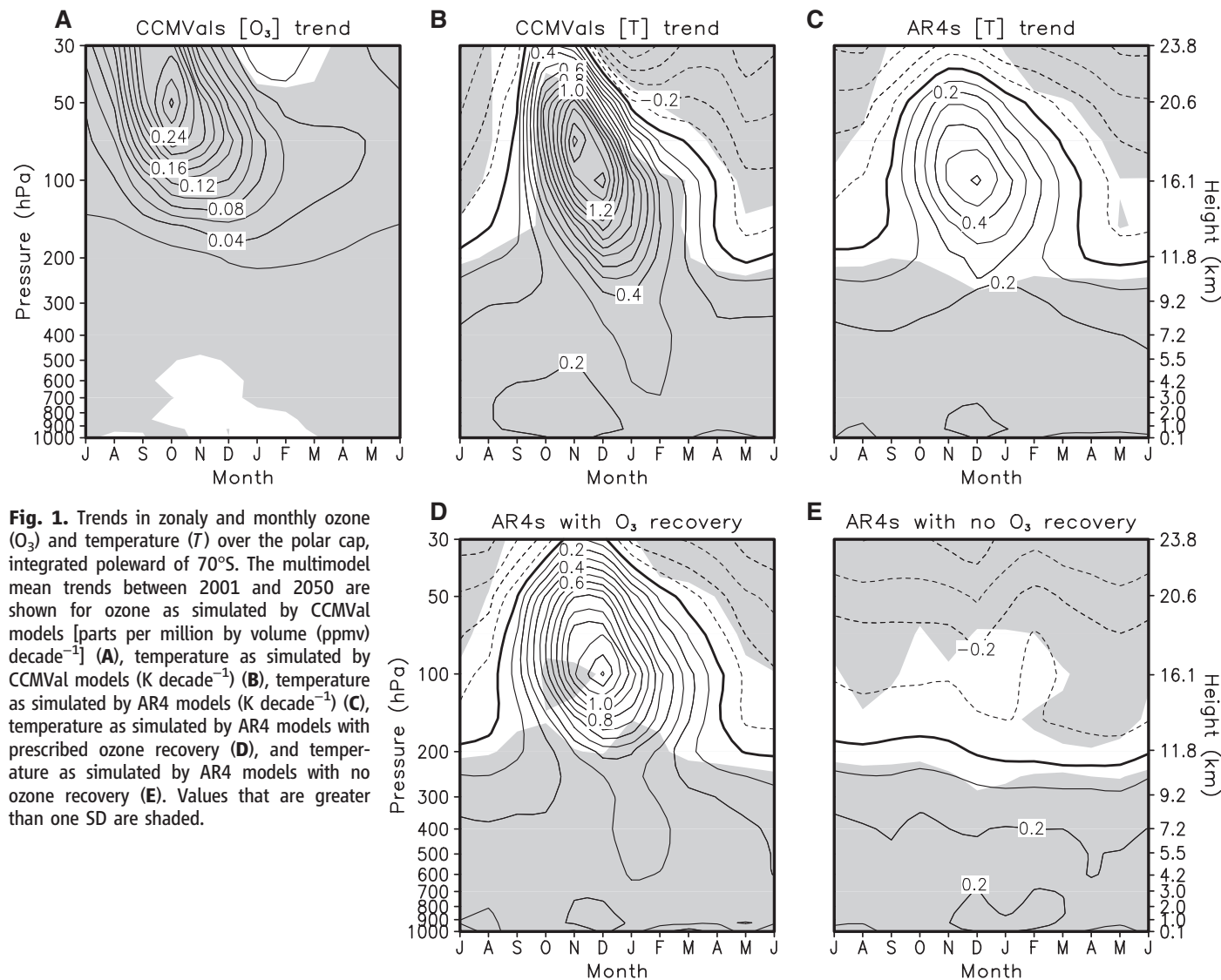
Fig. 1. Trends in zonaly and monthly ozone (O_3) and temperature (T) over the polar cap, integrated poleward of 70°S. The multimodel mean trends between 2001 and 2050 are shown for ozone as simulated by CCMVal models [parts per million by volume (ppmv) decade^{-1}] (**A**), temperature as simulated by CCMVal models (K decade^{-1}) (**B**), temperature as simulated by AR4 models (K decade^{-1}) (**C**), temperature as simulated by AR4 models with prescribed ozone recovery (**D**), and temperature as simulated by AR4 models with no ozone recovery (**E**). Values that are greater than one SD are shaded.

trend. Associated with such ozone recovery, lower-stratospheric temperatures over the polar cap increase substantially, as seen in Fig. 1B. This warming reaches down into the upper troposphere, as has been noted in stratospheric-resolving general circulation model experiments with pre-scribed ozone depletion (9) and chemistry-climate model integrations for the recent past (22).

Figure 1C shows corresponding polar-cap temperature trends, as predicted by all AR4 models. This multimodel mean trend shows a much weaker warming and is not statistically significant in the upper troposphere and lower stratosphere. This is due to the way in which ozone is prescribed in the AR4 models. In nearly half of those models, there is no ozone recovery, and this results in the absence of warming in the lower stratosphere for those models (Fig. 1E). Even when ozone recovery is prescribed (Fig. 1D), the AR4 models produce less robust polar-cap warming than the CCMVal models because of the large intermodel difference in temperature trends.

The ozone-induced temperature change in the lower-stratospheric polar cap has a substantial impact on the pressure and wind fields in the tropo-sphere below (2, 10, 11). Figure 2A shows the multimodel mean trend in December-to-February mean SH westerlies simulated by CCMVal mod-els. The tropospheric westerlies are found to be decelerated on the poleward side of the jet, imply-ing a negative trend in Southern annular mode index in the future. This result is opposite to the one predicted by the multimodel mean of AR4 models, which shows acceleration on the pole-ward side of the jet (Fig. 2B). The importance of ozone-related warming is even clearer if one compares AR4 models with and without a prescribed ozone recovery. As seen in Fig. 2C, the multimodel mean trend for the subset of AR4 integrations with ozone recovery exhibits features qualitatively similar to those in CCMVal models, although the dipolar pattern is weaker and does not reach to the surface. When the ozone recovery is neglected (Fig. 2D), the AR4 models predict the opposite trend in the extratropics. This result indicates that the effect of ozone-induced warming overwhelms that of greenhouse gas–induced cooling in the lower-stratospheric polar cap and plays an important role in the acceleration of the tropospheric westerlies during the SH summer. Note that, owing to its strong seasonality (Fig. 1A), ozone recovery plays a minimal role during other seasons (22).

The impact of stratospheric ozone recovery on the SH westerlies is further clarified in Fig. 3, where the relationships among trends in lower-stratospheric polar-cap ozone and temperature, as well as lower-tropospheric westerlies, are shown for all model integrations. For the westerlies, trends are quantified by $\Delta[u]$: the difference in the 850-hPa zonal wind at $\pm 10°$ from the latitude of maximum wind. This is very similar to computing the South-ern annular mode index (1) but is much simpler in practice.

First, note that the polar-cap warming in the lower stratosphere is linearly correlated with ozone recovery in the CCMVal models (Fig. 3A). A linear correlation is also found between trends in polar-cap temperature and in $\Delta[u]$ (Fig. 3B). This suggests that stronger polar-cap warming, asso-ciated with ozone recovery, results in a larger neg-ative $\Delta[u]$ trend. This is equivalent to the larger negative trend of the Southern annular mode index (i.e., an equatorward intensification of the jet).

Second, consider the corresponding plot for AR4 models (Fig. 3C). Although essentially no relationship is found between trends in polar-cap temperature and in $\Delta[u]$ for those AR4 models with no ozone recovery (open circles), a signif-icant negative correlation appears for those AR4 models with prescribed ozone recovery (filled circles). Moreover, the negative correlation for the latter AR4 models (dashed gray line) is sim-ilar to the one obtained from the CCMVal models (solid gray line). This shows that the response of tropospheric westerlies to polar-cap temperature trends is very robust, because it is found in two sets of substantially different climate models.

Third, observe that most CCMVal models show negative $\Delta[u]$ trends (Fig. 3B), whereas most AR4 models show positive $\Delta[u]$ trends (Fig. 3C), even when ozone recovery is prescribed. This difference is consistent with weaker polar-cap warming in AR4 models as compared with CCMVal models. Most AR4 models predict a polar-cap temperature trend smaller than ~ 1 K decade^{-1}, and such values result in a positive $\Delta[u]$ trend, even for the CCMVal models. At present, it is unclear why AR4 models underestimate the low-stratospheric polar-cap warming. On the one hand, it could result from an incorrect specifica-tion of the ozone recovery either in amplitude or spatial distribution (23); however, this cannot be ascertained, because the precise ozone fields used in each AR4 model have not been archived. On the other hand, it might result from the poorly resolved stratospheric circulation, the lack of ver-tical resolution, or artificial damping near the low model tops in AR4 models. Further work is needed to clarify this underestimate.

The detailed mechanisms through which stratospheric ozone affects the tropospheric west-erly jet remain unclear at present. Several hypothe-
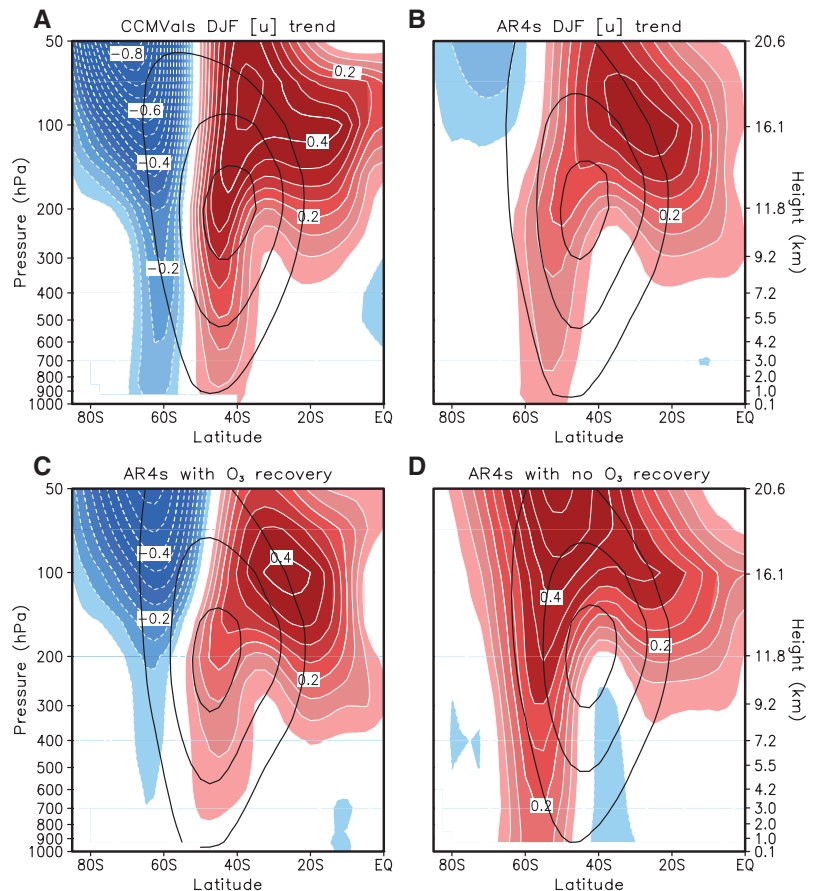

Fig. 2. Trends in December-to-February (DJF) zonal-mean zonal wind. The multimodel mean trends between 2001 and 2050 are shown for the CCMVal models (**A**), the AR4 models (**B**), the AR4 models with prescribed ozone recovery (**C**), and the AR4 models with no ozone recovery (**D**). Shading and contour intervals are 0.05 ms^{-1} decade^{-1}. Deceleration and acceleration are indicated with blue and red colors, respectively, and trends weaker than 0.05 ms^{-1} decade^{-1} are omitted. Superimposed black solid lines are DJF zonal-mean zonal wind averaged from 2001 to 2010, with a contour interval of 10 ms^{-1}, starting at 10 ms^{-1}. EQ, equator.

Fig. 3. Relationships among SH polar-cap ozone trend at 100 hPa, polar-cap temperature trend at 100 hPa, and extra-tropical zonal wind trend at 850 hPa: for ozone and temperature trends as simulated by CCMVal models (**A**), for zonal wind and temperature trends as simulated by CCMVal models (**B**), and for zonal wind and temperature trends as simulated by AR4 models (**C**). Here, ozone and temperature trends are calculated for September-to-December and November-to-January mean quantities, respectively. The averaging months are chosen to reflect the largest trends at 100 hPa, as seen in Fig. 1. The zonal wind trends at 850 hPa are quantified by $\Delta[u]$: the difference in DJF-averaged zonal wind at $\pm10°$ from the latitude of maximum wind. Negative values denote the deceleration (acceleration) of westerlies on the poleward (equatorward) side of the maximum wind. The filled and open circles in (C) correspond to the AR4 models with and without prescribed ozone recovery. Solid and dashed gray lines in (B) and (C) indicate linear fit for CCMVal models and AR4 models with prescribed ozone recovery, respectively. Numbers within parentheses in the key denote the number of ensemble members used for each model. dec., decade.
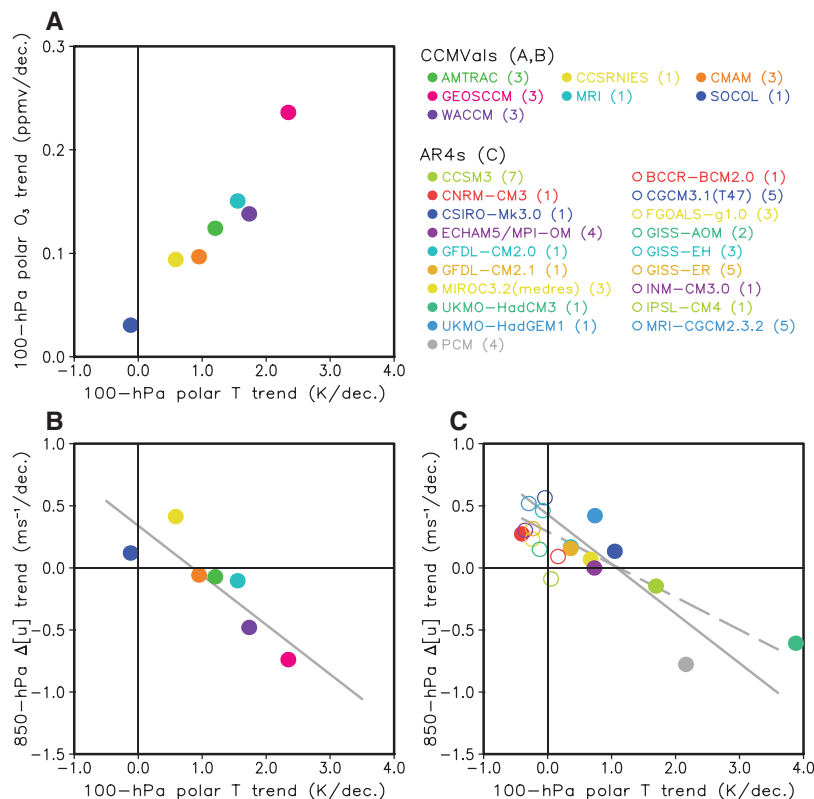
ses have been proposed (*4, 24–27*), but none have been validated or falsified. Nonetheless, our analyses suggest that stratospheric processes, and ozone recovery in particular, may be able to affect SH climate in major ways and thus should be included in predictions of SH climate in the 21st century.

References and Notes

1. D. W. J. Thompson, J. M. Wallace, G. C. Hegerl, *J. Clim.* **13**, 1018 (2000).
2. D. W. J. Thompson, S. Solomon, *Science* **296**, 895 (2002).
3. G. J. Marshall, *J. Clim.* **16**, 4134 (2003).
4. G. Chen, I. Held, *Geophys. Res. Lett.* **34**, L21805 (2007).
5. J. H. Yin, *Geophys. Res. Lett.* **32**, L18701 (2005).
6. J. Lu, G. A. Vecchi, T. Reichler, *Geophys. Res. Lett.* **34**, L06805 (2007).
7. J. Russell, K. W. Dixon, A. Gnanadesikan, R. J. Stouffer, J. R. Toggweiler, *J. Clim.* **19**, 6382 (2006).
8. B. K. Mignone, A. Gnanadesikan, J. L. Sarmiento, R. D. Slater, *Geophys. Res. Lett.* **33**, L01604 (2006).
9. N. P. Gillett, D. W. J. Thompson, *Science* **302**, 273 (2003).
10. D. T. Shindell, G. A. Schmidt, *Geophys. Res. Lett.* **31**, L18209 (2004).
11. J. M. Arblaster, G. A. Meehl, *J. Clim.* **19**, 2896 (2006).
12. A first hint of ozone recovery is already present in the most recent observations (*15, 28*). The sharp decrease in stratospheric ozone concentration has ceased around the year 2000, and ozone levels have started to increase since then. Although weak, this increasing trend is found in almost all ground-based and satellite observations (*28*). In addition, the chemistry-climate models, discussed in the text, predict that the increase in stratospheric ozone concentration will continue in the 21st century (*15*).
13. R. L. Miller, G. A. Schmidt, D. T. Shindell, *J. Geophys. Res.* **111**, D18101 (2006).
14. D. J. Lorenz, E. T. DeWeaver, *J. Geophys. Res.* **112**, D10119 (2007).
15. V. Eyring *et al.*, *J. Geophys. Res.* **112**, D16303 (2007).
16. The CCMVal models used in this study are AMTRAC, CCSRNIES, CMAM, GEOSCCM, MRI, SOCOL, and WACCM

[see table 1 of (*15*) for the detailed model configuration]. All available ensemble members are used for each model.
17. G. A. Meehl *et al.*, in *Climate Change 2007: The Physical Science Basis. Contribution of Working Group I to the Fourth Assessment Report of the Intergovernmental Panel on Climate Change* (Cambridge Univ. Press, Cambridge, 2007), pp. 747–845.
18. E. C. Cordero, P. M. de F. Forster, *Atmos. Chem. Phys.* **6**, 5369 (2006).
19. The AR4 models used in this study are BCCR-BCM2.0, CCSM3, CGCM3.1(T47), CNRM-CM3, CSIRO-Mk3.0, ECHAM5/MPI-OM, FGOALS-g1.0, GFDL-CM2.0, GFDL-CM2.1, GISS-AOM, GISS-EH, GISS-ER, INM-CM3.0, IPSL-CM4, MIROC3.2(medres), MRI-CGCM2.3.2, UKMO-HadCM3, UKMO-HadGEM1, and PCM. Among these 19 models, 10 models—CCSM3, CNRM-CM3, CSIRO-Mk3.0, ECHAM5/MPI-OM, GFDL-CM2.0, GFDL-CM2.1, MIROC3.2(medres), UKMO-HadCM3, UKMO-HadGEM1, and PCM—prescribe ozone recovery. All available ensemble members are used for each model.
20. Changes in stratospheric ozone concentration in CCMVal model integrations are not perfectly linear. Almost all CCMVal models predict a slow increase until 2010 and a relatively faster increase thereafter until about 2060 [see figure 7 in (*15*)].
21. W. Randel, F. Wu, *Geophys. Res. Lett.* **26**, 3089 (1999).
22. J. Perlwitz, S. Pawson, R. L. Fogt, J. E. Nielsen, W. D. Neff, *Geophys. Res. Lett.* **35**, L08714 (2008).
23. J. A. Crook, N. P. Gillett, S. P. E. Keeley, *Geophys. Res. Lett.* **35**, L07806 (2008).
24. D. T. Shindell, G. A. Schmidt, R. L. Miller, D. Rind, *J. Geophys. Res.* **106**, 7193 (2001).
25. J. Perlwitz, N. Harnik, *J. Clim.* **16**, 3011 (2003).
26. P. J. Kushner, L. M. Polvani, *J. Clim.* **17**, 629 (2004).
27. D. W. J. Thompson, J. C. Furtado, T. G. Shepherd, *J. Atmos. Sci.* **63**, 2616 (2006).
28. E.-S. Yang, D. M. Cunnold, M. J. Newchurch, R. J. Salawitch, *Geophys. Res. Lett.* **32**, L12812 (2005).
29. The authors thank J. Austin and J. Perlwitz for helpful discussions and suggestions on the manuscript, the National Oceanic and Atmospheric Administration Climate Diagnostics Center for providing the National Centers for Environmental Prediction–NCAR reanalysis data, the European Centre for Medium-Range Weather Forecasts for providing the ERA40 data, the World Climate Research Programme SPARC CCMVal project for organizing the chemistry-climate model (CCM) data analysis activity, the British Atmospheric Data Center for collecting and archiving the CCM output, the Program for Climate Model Diagnosis and Intercomparison for collecting and archiving the IPCC/AR4 model data, the Joint Scientific Committee of the Climate Variability Working Groups on Coupled Modeling and their Coupled Model Intercomparison Project and Climate Simulation Panel for organizing the model data analysis activity, and the IPCC Working Group I Technical Support Unit for technical support. The IPCC Data Archive at the Lawrence Livermore National Laboratory is supported by the Office of Sciences, U.S. Department of Energy. The work of S.W.S. and L.M.P. is supported, in part, by a grant from the NSF. Contributions of D.W.W. and S.P. are supported by NASA's modeling and analysis program, and GEOSCCM was run on Columbia with resources allocated by NASA's high-performance computing program. WACCM simulations were carried out at NCAR, at NASA's Ames Research Center, and at the Barcelona Supercomputing Center, Spain. The CCSRNIES's research is supported by the Global Environmental Research Fund of the Ministry of the Environment of Japan (A 071) and a grant in aid for scientific research from the Ministry of Education, Culture, Sports, Science and Technology of Japan (no. 19340138). The development and maintenance of SOCOL are supported by ETH Zurich (grant PP 1/04 1) and the Swiss National Science Foundation (grant SCOPES IB7320 110884). Contributions of the CMAM group and T.G.S. are supported by the Canadian Foundation for Climate and Atmospheric Sciences, the Natural Sciences and Engineering Research Council of Canada, and Environment Canada. NCAR is sponsored by the NSF.